Journal of Power Sources, 50 (1994) 67–79

Effect of gelling on the electrode kinetics of the $Pb/PbSO_4$ and hydrogen-electrode reactions in maintenance-free lead/acid batteries

M.P. Vinod and K. Vijayamohanan*
Materials Chemistry Division, National Chemical Laboratory, Pune-411 008 (India)

(Received July 13, 1993; accepted November 17, 1993)

Abstract

The electrode kinetics of the $Pb/PbSO_4$ and the hydrogen-evolution reactions on porous lead electrodes in sulfuric acid has been studied using a quantitative analysis of galvanostatic transients in the linear polarization domain. Significant changes are observed in the kinetics with the addition of thixotropic agents (e.g., sodium silicate) that are often employed in the manufacture of maintenance-free lead/acid batteries. The effects of these thixotropic agents on the charge-transfer and ohmic components of the $Pb/PbSO_4$ reaction and charge-transfer components of hydrogen-electrode reaction are analysed with the help of a 'pore-plugging' model. This study allows a non-destructive determination of the electrode kinetic parameters and the internal resistance contribution from pore-plugging. This is useful when designing maintenance-free lead/acid batteries.

Introduction

The advent of sealed maintenance-free batteries in recent years has resulted increasingly in the use of immobilized and absorbed electrolytes [1–3], with or without catalytic recombination plugs. In the former, the loss of oxygen and hydrogen (produced during charge or overcharge of the respective positive and negative electrode) is minimized either by oxygen/hydrogen recombination on a suitable catalyst in the vent plug, or by oxygen reduction on the porous lead of the negative electrode. In the latter, immobilization of the electrolyte is necessary and is achieved by adding a thixotropic agent, such as sodium silicate, to the electrolyte. Addition of a thixotropic agent will, however, have other implications, such as: increased ohmic resistance; changes in the interfacial kinetics due to adsorption of silicate ions; formation of cracks in the electrolyte, and gas entrapment. Furthermore, a progressive loss of hydrogen from the cell can cause drying out of the gel and results in electrolyte imbalance followed by eventual cell or battery failure. Although pressure-regulated valve cells with gelled electrolyte are commonly used for several float applications, none of the above problems have been systematically analysed, except for the effect of thixotropic agents on the kinetics of hydrogen evolution [4]. More importantly, recent studies [5, 6] indicate that the lead/acid system is amenable to pulsed discharge. Such operation demands a careful analysis of the effect of gelling on the ohmic drop (IR), especially if maintenance-free gelled systems are to be used for these and other

*Author to whom correspondence should be addressed.

0378-7753/94/$07.00 © 1994 Elsevier Sequoia. All rights reserved
SSDI 0378-7753(93)01883-J

high-rate applications. Addition of silicate ions is also known to cause favourable changes in the shelf life and the cycle life of lead/acid batteries.

In this paper a study of the kinetics of the lead electrode and the hydrogen-electrode reactions in gelled and non-gelled electrolyte systems is presented. Within the range of open-circuit potentials observed for the $Pb/PbSO_4$ system, the hydrogen-evolution reaction (HER) can be considered to be in the Tafel domain and the lead electrode reaction to be operating in a quasi-reversible manner. Accordingly, the galvanostatic transients of the $Pb/PbSO_4$ electrode in gelled and non-gelled electrolyte have been analysed quantitatively in the linear polarization domain. From inspection of the build-up and decay regions of the transients, several useful parameters have been obtained, i.e., the double-layer capacitance and the exchange-current density of both the lead and the hydrogen-electrode reactions. More specifically, the plugging of the pores of the $Pb/PbSO_4$ electrode (due to the accumulation of the discharged products, $PbSO_4$), that results in a high IR drop has also been incorporated as a parameter in the analysis. The progressive variation of this parameter with battery state-of-charge (SOC) has been used to account for the pore plugging, a phenomenon that is known to limit the capacity of battery electrodes [6, 7]. Changes in pore-plugging that take place with gelling at a low SOC have also been evaluated. Note, any local alkalization in the pores that promotes the formation of PbO, as discussed by Pavlov [8, 9], is neglected in the present analysis.

Experimental

Negative and positive pasted plates (5.5 cm × 3 cm × 0.1 cm) were prepared using procedures described elsewhere [10]. All the plates used the same grid alloy, namely, Pb–0.08wt.%Ca–0.5wt.%Sn. Negative-limited cells, each with an excess of sulfuric acid (4.8 M) electrolyte, were assembled by placing a positive counter electrode (PbO_2) on either side of the negative working electrode, alongwith a Hg/Hg_2SO_4, H_2SO_4 (4.8 M) reference electrode. The reference electrode was connected to the test cell via a Luggin capillary that was aligned close to the working electrode in order to minimize the uncompensated resistance due to the solution. The potentials were measured with an accuracy of ± 1 mV by connecting a buffer amplifier with unity gain and high input impedance (10^{13} Ω) between the reference and working electrodes. All experiments were performed at a temperature of 25 ± 1 °C.

Initially, each electrode was soaked in 4.8 M H_2SO_4 for 10 h and then subjected to galvanostatic charging and discharging at the $C/10$ and the $C/8$ rate, respectively. This was continued for five cycles to stabilize the measured capacity value. The resulting constant value was used for all SOC calculations. (Note, SOC is defined as the ratio of available capacity of the electrode to the maximum available capacity.) All the cells were then given the same amount of overcharge (20%), kept at open circuit for 30 min, and polarized with appropriate current densities such that a steady state could be obtained in few minutes within the linear polarization range. On attaining the steady state, the current was interrupted and the open-circuit potential versus time transients were measured until the original equilibrium value was restored. The experiments were repeated using various current densities selected on the basis of those that caused negligible change in SOC (i.e. $\int I dt \ll \Delta SOC$).

Galvanostatic potential–time transients were obtained at various SOC values (i.e., 1, 0.5 and 0.05) by keeping the current densities at constant values. Similar experiments were conducted with separate electrodes at various SOC values and current densities

in an immobilized electrolyte. The latter was prepared by using sodium silicate (5 g l^{-1}) as a thixotropic agent [11, 12].

Results and discussion

Data for potential–time transients taken at various current densities in the linear polarization domain for gelled and non-gelled electrolytes at unit SOC are presented in Figs. 1 and 2, respectively. During both cathodic and anodic polarization, the build-up and decay transients were followed until a steady state was reached with an overpotential of less than 10 mV. This ensured a linear polarization domain. Similar plots for a low SOC value (0.05) are shown in Figs. 3 and 4 for gelled and non-gelled electrolytes, respectively. In each case, the potential tends to reach the steady-state

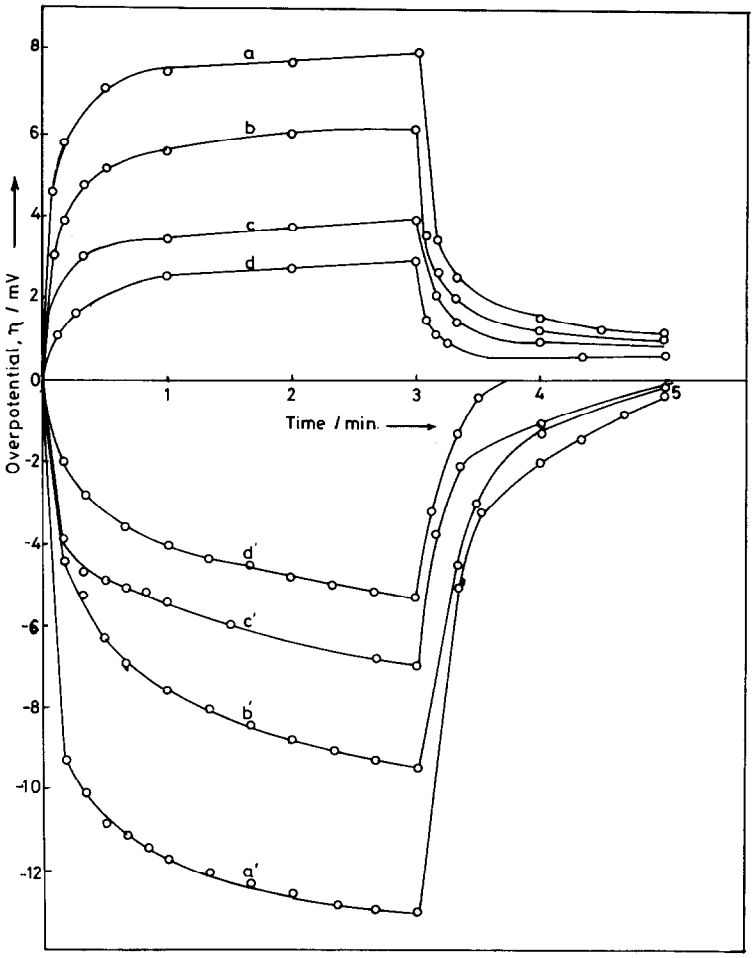

Fig. 1. Galvanostatic potential–time transients at various current densities in non-gelled electrolyte at SOC = 1: (a), (b), (c) and (d) correspond to anodic transients and (a'), (b'), (c') and (d') to cathodic transients at 60, 45, 30 and 15 μA cm^{-2}, respectively.

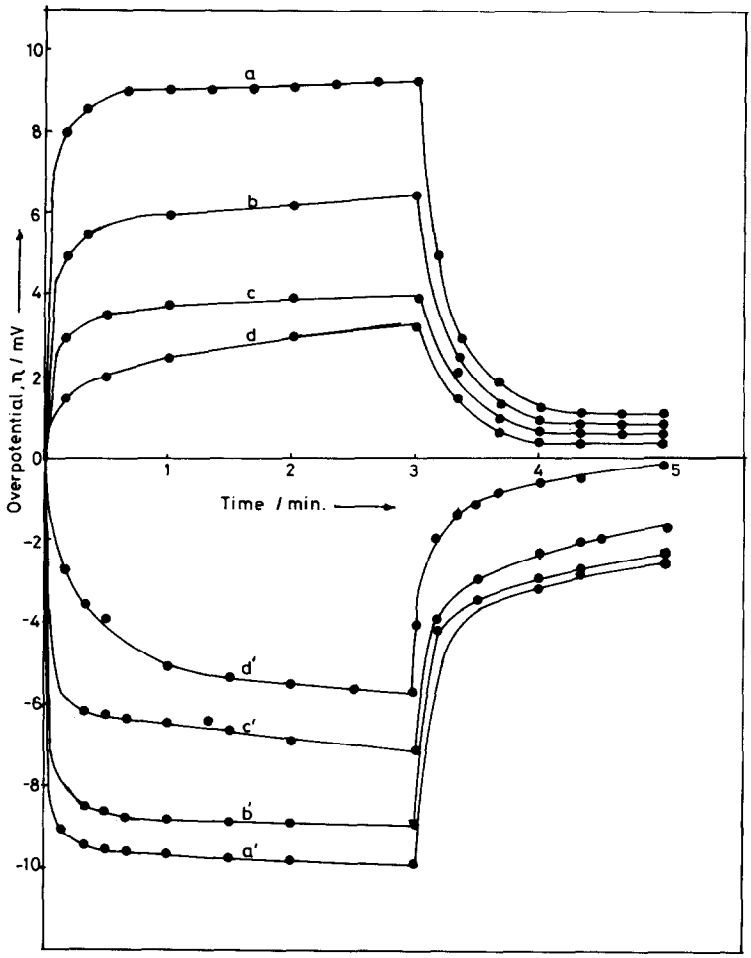

Fig. 2. Galvanostatic potential–time transients at various current densities for gelled electrolyte at SOC=1: (a), (b), (c) and (d) correspond to anodic transients and (a'), (b'), (c') and (d') to cathodic transients at 60, 45, 30 and 15 μA cm^{-2}, respectively.

value asymptotically with time; the time is longer for greater current densities. Significant differences can be observed between the cathodic and anodic transients at a given SOC value. Moreover, the transient patterns are less steep for a low SOC value, irrespective of the nature of the polarization. For cathodic polarization at a unit SOC value, the pattern is different from that of the other curves. This deviation can be attributed to the contribution of the HER on the electrode kinetics; this is insignificant at low SOC values. By contrast, noticeable changes are observed in the anodic patterns at a SOC of 0.05. This indicates the importance of the ohmic drop that arises from the accumulation of insulating $PbSO_4$ in the pores of the electrode.

The transient pattern in the gelled electrolyte is basically the same as that obtained in non-gelled electrolyte. At a given SOC, the build-up and decay transients are, however, much steeper for the gelled electrolyte. This can be attributed to the increased hindrance to mass transfer that is brought about by the presence of an interpenetrating

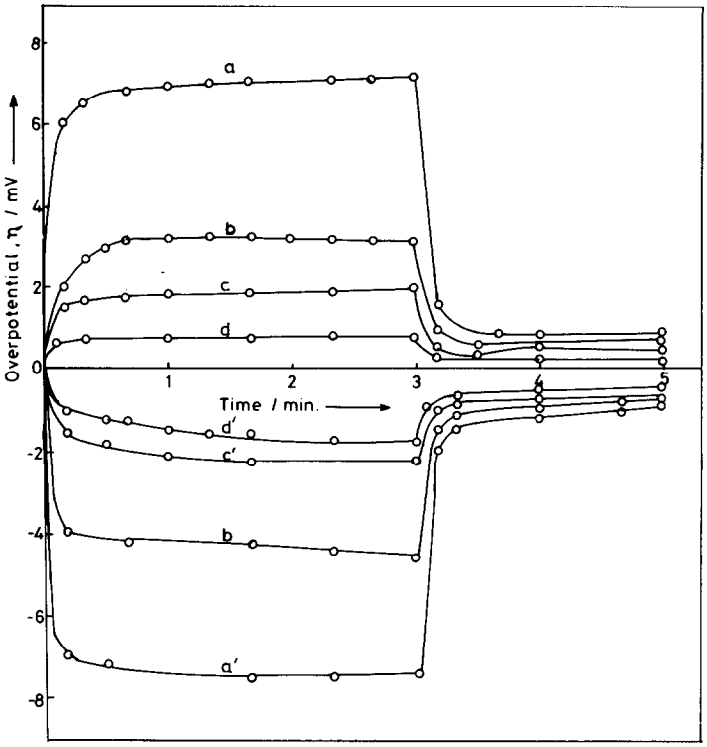

Fig. 3. Galvanostatic potential–time transients at various current densities for non-gelled electrolyte at SOC = 0.05: (a), (b), (c) and (d) correspond to anodic transients and (a'), (b'), (c') and (d') to cathodic transients at 60, 45, 30 and 15 μA cm^{-2}, respectively.

network of polysilicic acid gel. Variation of the transient pattern with the SOC is also observed with gelled electrolyte. The explanation for this behaviour is the same as that discussed above for non-gelled electrolyte.

Phenomenological model for galvanostatic transients

Various electrochemical reactions are reported to occur on a $Pb/PbSO_4$ electrode at open circuit [9]. Among these, the major potential-determining reactions are:

$$PbSO_4 + 2e^- \longrightarrow Pb + SO_4^{2-} \quad (1)$$

$$2H^+ + 2e^- \longrightarrow H_2 \quad (2)$$

$$O_2 + 4H^+ + 4e^- \longrightarrow 2H_2O \quad (3)$$

The respective reversible potentials of these reactions in 4.8 M sulfuric acid are −0.9716, −0.6186 and +0.6116 V versus a Hg/Hg_2SO_4, H_2SO_4 reference electrode. Among these reactions, the oxygen-reduction reaction can be neglected due to the following kinetic reasons. The dissolution of oxygen from the atmosphere and its supply to the electrode surface by diffusion is a relatively slow process in a quiescent solution. More importantly, a constant evolution of hydrogen, as observed experimentally at

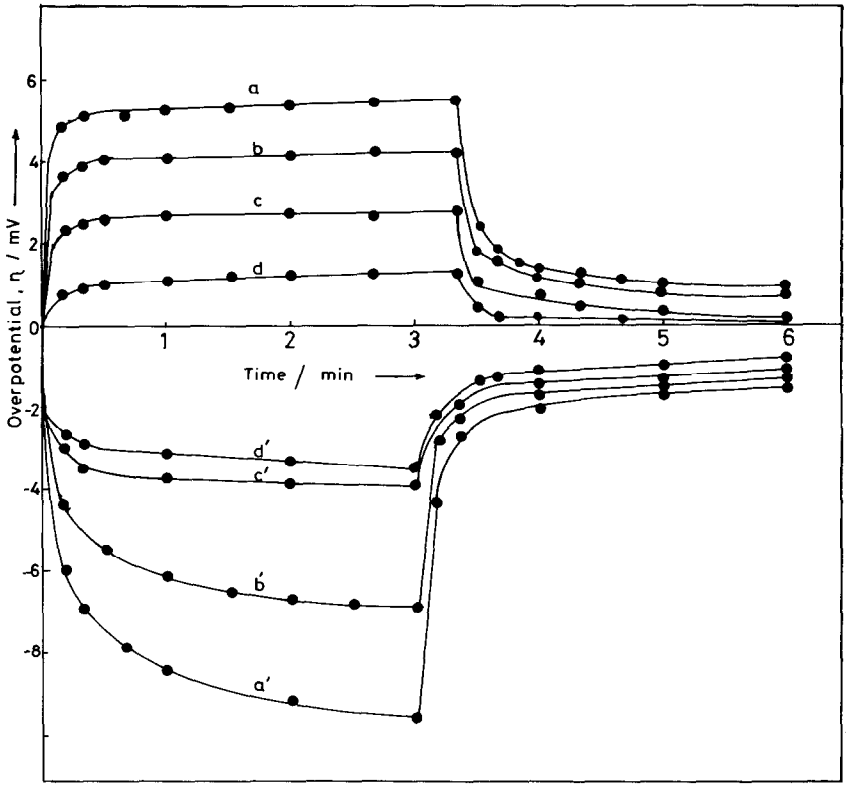

Fig. 4. Galvanostatic potential–time transients at various current densities for gelled electrolyte at SOC=0.05: (a), (b), (c) and (d) correspond to anodic transients and (a'), (b'), (c') and (d') to cathodic transients at 60, 45, 30 and 15 μA cm^{-2}, respectively.

open circuit, will make the electrolyte likely to be saturated with hydrogen in the beginning, especially at high SOC values. Hence, the general current–potential relation for the remaining two reactions can be written as:

$$I = -C_{dl}(dE/dt) + I_{0,Pb}[\exp(-\alpha_{Pb} f \eta_{Pb}) - \exp(\beta_{Pb} f \eta_{Pb})] + I_{0,H}[\exp(-\alpha_H f \eta_H) - \exp(\beta_{Pb} f \eta_H)] \quad (4)$$

Where, the first term corresponds to the non-faradaic current with C_{dl} as the double-layer capacitance; the second and third terms correspond to faradaic currents associated with eqns. (1) and (2), respectively; η_{Pb} and η_H are the overpotentials for eqns. (1) and (2) defined as $E - E_{Pb}{}^r$ and $E - E_H{}^r$, respectively; $I_{0,Pb}$ and $I_{0,H}$ are the corresponding exchange-current densities; α_{Pb}, β_{Pb}, α_H and β_H are the apparent charge-transfer coefficients for the associated reactions; f is given by nF/RT, with n as the number of electrons involved in the respective rate-determining steps.

Equation (4) is valid only if mass-transfer polarization can be considered as negligible for the faradaic reactions. A high concentration of sulfuric acid (4.8 M) and invariance of transients with stirring justifies this assumption. In addition, the time-dependent diffusional contributions are rendered insignificant by a judicious choice of experimental conditions. The current density is selected to be extremely small

(approximately $C/500$, where C is the nominal capacity of the electrode) for a duration of only few minutes. These two criteria imply that the diffusional polarization is negligibly small compared with the charge-transfer and the ohmic components, even at the end of each experiment. This can be further supported by the following approximate calculation.

In the linear polarization domain, the magnitude of the diffusional polarization is given approximately by $(RT/nF)\ \ln(1-I/I_L)$, where I_L is the instantaneous limiting current. This limiting current could be as high as the $20C$ rate, or perhaps the short-circuit current for charged lead/acid batteries [13]. The diffusional polarization is therefore less than few microvolts (i.e., $<0.05\%$) in the experiments performed here. A close examination of the observed potential–time transients reveals that the HER could occur irreversibly in the linear polarization domain of the $Pb/PbSO_4$ electrode. Hence, for overpotentials <10 mV, eqn. (4) can be written as:

$$I = -C_{dl}(dE/dt) - I_{0,Pb}[(\alpha_{Pb}+\beta_{Pb})f(E-E_{Pb}^{r})] + I_{0,H}[\exp(-\alpha_H f(E-E_H^{r}))] \quad (5)$$

This equation includes the quasi-reversible nature of $Pb/PbSO_4$ reaction, along with the charge-transfer components of the HER in a Tafel domain. Simplification of eqn. (5) yields:

$$I = -C_{dl}(dE/dt) - I_{0,Pb}\gamma f(E-E_{Pb}^{r}) + I_{0,H}[\exp(-\alpha_H f(E-E_H^{r}+E_{Pb}^{r}-E_{Pb}^{r}))] \quad (6)$$

where, $\gamma=(\alpha_{Pb}+\beta_{Pb})$. Equation (6) can be written as:

$$I = -C_{dl}(dE/dt) - I_{0,Pb}\gamma f(E-E_{Pb}^{r}) + [\exp(-\alpha_H f(E_{Pb}^{r}-E_H^{r}))]Q \quad (7)$$

with Q as a constant defined as $I_{0,H}\ \exp[(-\alpha_H f(E-E_{Pb}^{r}))]$. Thus:

$$I = -C_{dl}(dE/dt) - I_{0,Pb}\gamma f(E-E_{Pb}^{r}) + Q[1-\alpha_H f(E-E_{Pb}^{r})] \quad (8)$$

On simplification, eqn. (8) yields:

$$I = -C_{dl}(dE/dt) - \alpha f(E-E_{Pb}^{r})(I_{0,Pb}+\alpha_H Q) + Q \quad (9)$$

Generally, for porous battery electrodes, as the SOC decreases during discharge, the ohmic resistance of accumulated products in the pores progressively increases. The latter is known to limit the capacity [6, 7]. In such a situation, the ohmic component is a significant parameter to be considered while designing porous electrodes for high-rate applications. This is of marked importance in the case of maintenance-free of battery electrodes (especially for those with immobilized electrolytes) as one of the key features to be optimized is the ohmic drop due to the non-conducting materials ($PbSO_4$ alongwith the gell) inside the pores. The observed electrode potential E, with correction for this porous electrode resistance R_0, would be $(E+IR_0)$. The factor R_0 will depend only on the SOC of the electrode along with any changes that are induced by electrolyte immobilization. Hence,eqn. (9) can be recast as:

$$I = -C_{dl}d(E+IR_0)/dt - \gamma f(E-E_{Pb}^{r}+IR_0)[(I_{0,Pb}+\alpha_H Q)+Q \quad (10)$$

This expression can be taken as the governing equation for both the build-up and the decay transients of the $Pb/PbSO_4$ system in the linear polarization domain, which includes the charge-transfer and ohmic components of the lead electrode reaction together with the charge-transfer polarization of the HER. Since R_0 is assumed to vary only with SOC, eqn. (10) can be used generally to analyse the above two components

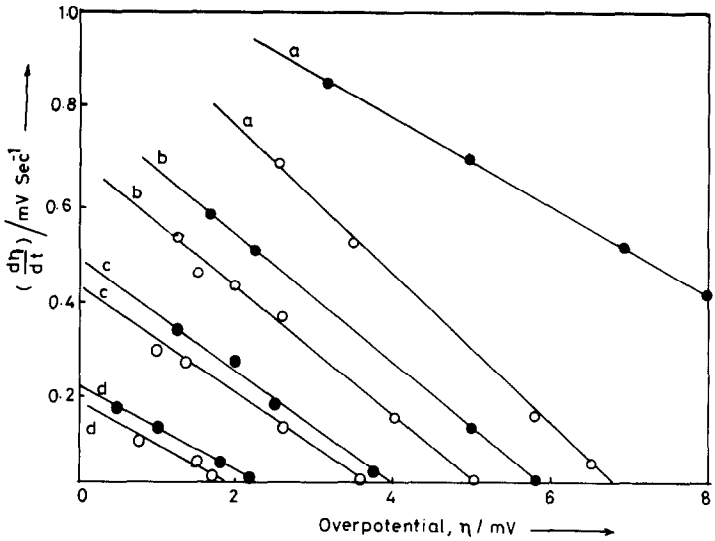

Fig. 5. Plot of dE/dt vs. η for non-gelled and gelled electrolyte as derived from the anodic transients at unit SOC using the data from Figs. 1 and 2: (○) and (●) indicate non-gelled and gelled electrolyte, respectively.

of the electrode kinetics. By taking $K = \gamma f(I_{0,\mathrm{Pb}} + \alpha_{\mathrm{H}} Q)$, at any SOC, and since R_0 is a constant, eqn. (10) can be written as:

$$I = -C_{\mathrm{dl}}\mathrm{d}(E + IR_0)/\mathrm{d}t - (E - E_{\mathrm{Pb}}{}^{\mathrm{r}} + IR_0)K + Q \tag{11}$$

on rearranging:

$$I = -C_{\mathrm{dl}}/(1 + KR_0)(\mathrm{d}E/\mathrm{d}t) - K(E - E_{\mathrm{Pb}}{}^{\mathrm{r}})/(1 + KR_0) + Q/(1 + KR_0) \tag{12}$$

This expression contains two unknowns (namely, R_0 and K) and can be solved using the following strategy. If at a particular SOC value two different values of current are taken (i.e., I' and I''), one of which is zero and corresponds to open-circuit conditions, two equations can be formulated as follows:

$$I' = -C_{\mathrm{dl}}/(1 + KR_0)(\mathrm{d}E'/\mathrm{d}t) - K(E' - E_{\mathrm{Pb}}{}^{\mathrm{r}})/(1 + KR_0) + Q/(1 + KR_0) \tag{13}$$

$$I'' = -C_{\mathrm{dl}}/(1 + KR_0)(\mathrm{d}E''/\mathrm{d}t) - K(E'' - E_{\mathrm{Pb}}{}^{\mathrm{r}})/(1 + KR_0) + K/(1 + KR_0) \tag{14}$$

By comparing the slopes of the decay and build-up transients at the same potential (i.e., $E' = E''$), the magnitude of the $C/(1 + KR_0)$ can be calculated from eqns. (13) and (14), i.e.:

$$C/(1 + KR_0) = \mathrm{I}' - \mathrm{I}''/(\mathrm{d}E'/\mathrm{d}t) - (\mathrm{d}E''/\mathrm{d}t) \tag{15}$$

Using these $C/(1 + KR_0)$ values, the double-layer capacitance can be calculated from eqn. (11), which on rearranging gives:

$$C_{\mathrm{dl}}(dE/\mathrm{d}t) = -I(1 + KR_0) - K(E - E_{\mathrm{Pb}}{}^{\mathrm{r}}) + Q \tag{16}$$

Therefore, if $(\mathrm{d}E/\mathrm{d}t)$ is plotted against $E - E_{\mathrm{Pb}}{}^{\mathrm{r}}$, a straight line should be obtained with a slope of $-K/C$ and an intercept of $[Q - I(1 + KR_0)]/C$. Furthermore, C and K can be calculated by using the exchange-current density and Tafel slopes that have

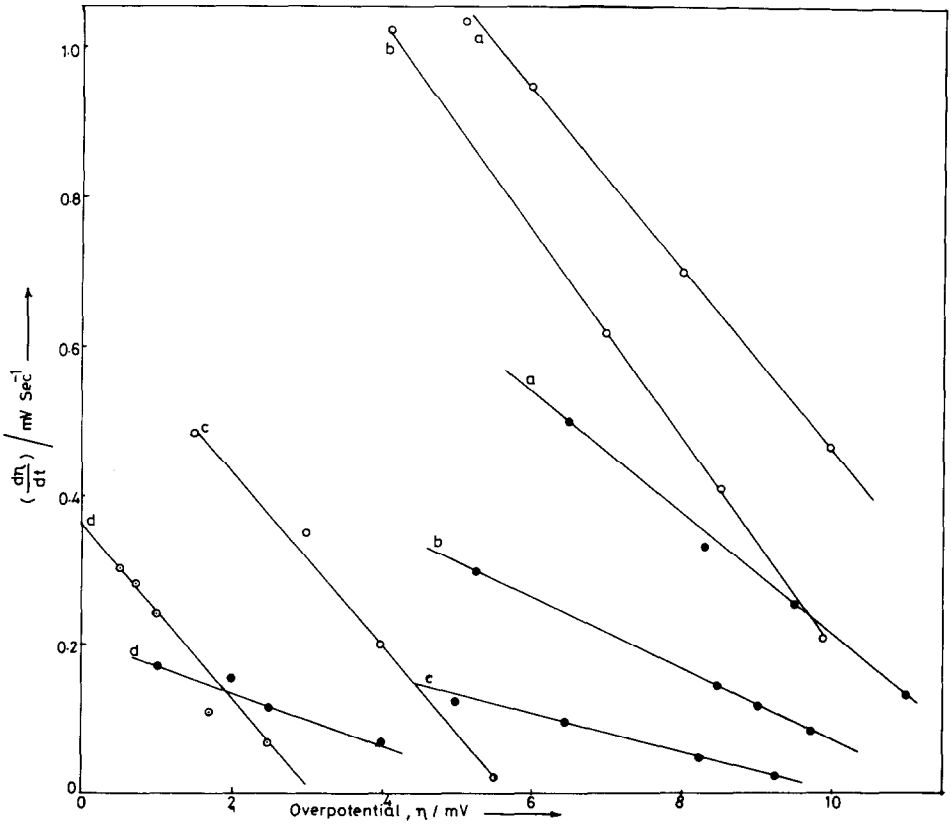

Fig. 6. Plot of dE/dt vs. η for (○) non-gelled and (●) gelled electrolyte as derived from the anodic transients at SOC=0.5. Current density: (a) 60; (b) 45; (c) 30 and (d) 15 μA cm^{-2}.

been reported [4, 14] for the HER on porous lead electrodes. It is especially useful to compute R_0 and the exchange-current density of the $Pb/PbSO_4$ reaction at various SOC values. The variation in R_0 and C_{dl} at fixed SOC values can now be correlated to the effect of gelling. The resulting data could be useful for the design of maintenance-free lead/acid batteries.

Comparison of theory with experimental data

Figures 5 to 8 show dE/dt versus η plots for gelled and non-gelled electrolytes at three representative SOC values, namely, 1, 0.5 and 0.05. The linearity shown in all the cases is in excellent agreement with the model suggested by eqn. (16). Furthermore, the slopes and intercepts of these curves provide estimates of R_0 with known $C/(1+KR_0)$ values. Given the large number of data points and the range as well as the direction of the current, the mean deviation of about +2% in each case suggests that the $C/(1+KR_0)$ values are fairly reliable.

The double-layer capacitance, exchange-current density and R_0 thus calculated are given in Table 1. The double-layer capacitance values remain unchanged with

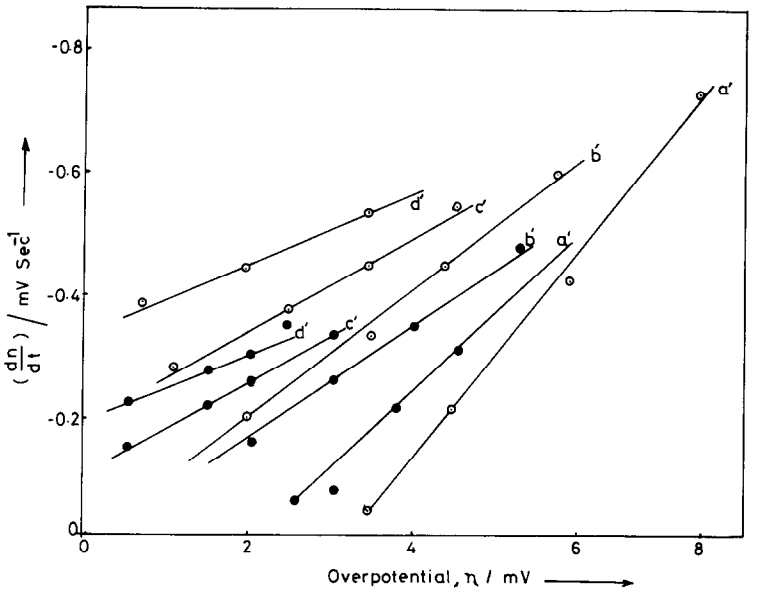

Fig. 7. Plot of dE/dt vs. η for (○) non-gelled and (●) gelled electrolyte as derived from cathodic transients at SOC = 0.5. Current density: (a') 60; (b') 45; (c') 30, and (d') 15 μA cm^{-2}.

respect to gelling for a given SOC value. This probably indicates the absence of any specific adsorption of silicate ions; the change of capacitance with SOC is more prominent, but the area change and the potential-dependent adsorption-pseudo-capacitance may play a complex role to cause this. For gelled electrolyte, the $I_{0,\mathrm{Pb}}$ value exhibits a gradual decrease at a particular SOC. This may be attributed to the increased contribution of diffusional resistance in the presence of gelling.

Although the magnitude of C_{dl} in Table 1 appears to be larger than the usual values for metal/solution interfaces, it is quite possible that the surface roughness factor associated with porous electrodes causes this deviation. Considering a medium value for the surface area of a few m^2 g^{-1} and a 10^3 to 10^4 increase in the apparent area due to porosity [7], the double-layer capacitance can be estimated to be 6 to 60 μF cm^{-2}. This value is close to those reported for lead in sulfuric acid [14].

In contrast to both $I_{0,\mathrm{Pb}}$ and C_{dl}, the ohmic resistance (R_0) in Table 1 shows a significant variation due to gelling as well as to SOC change. Addition of thixotropic agents obviously increases the ohmic drop and this effect is more pronounced at a low SOC, such as 0.05. Furthermore, the variation of R_0 with SOC can be attributed to the increased hindrance of charge transfer as a result of accumulation of insulating $PbSO_4$ in the pores of the electrode. The gelled electrolyte with SOC = 0.05 gives the highest value of ohmic resistance due to pore-plugging (namely, 415 Ω) and, hence, is unsuitable for deep-discharge applications.

The above results confirm the importance of ohmic drop due to pore-plugging. This aspect is general for all types of porous electrodes. Since most battery electrodes are porous in nature, the above analysis is helpful in estimating the extent of pore-plugging without any *a priori* assumptions regarding the detailed geometry of the porous electrode. Moreover, R_0 has special significance in designing maintenance-free

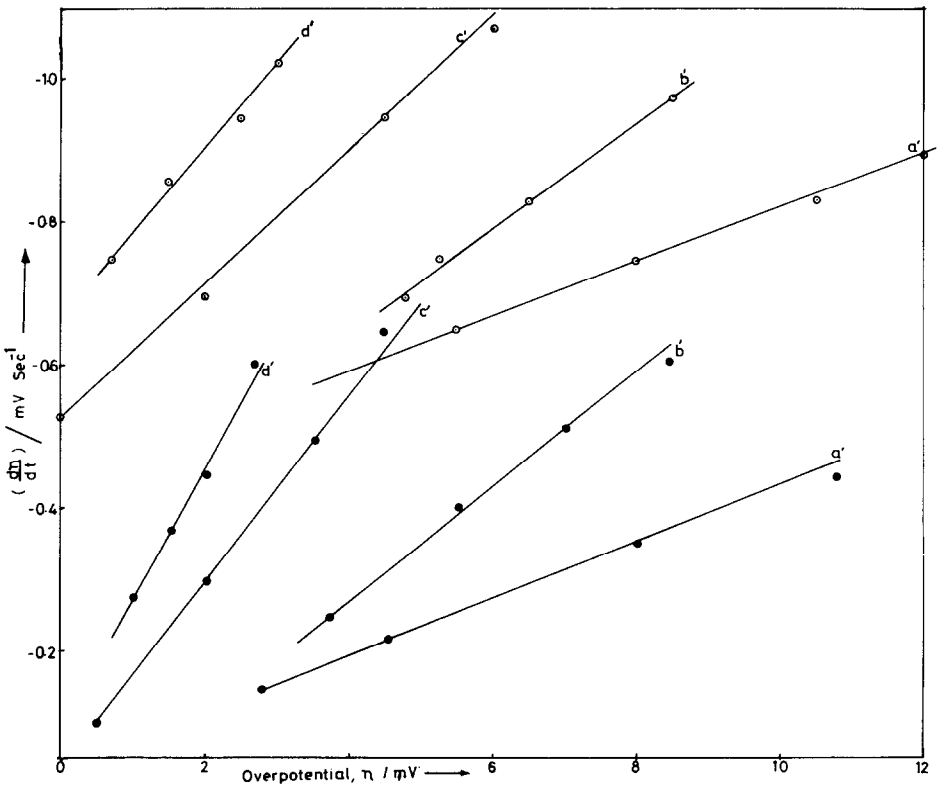

Fig. 8. Plot of dE/dt vs. η for (○) non-gelled and (●) gelled electrolyte as derived from cathodic transients at SOC=0.05 using data from Figs. 3 and 4.

TABLE 1

Double-layer capacitance (C_{dl}), exchange-current densities ($I_{0,Pb}$) and ohmic resistance for gelled and non-gelled $Pb/PbSO_4$ system at different states-of-charge (SOCs)

Electrode type polarization	SOC	C_{dl}[a] (F cm^{-2})	$I_{0,Pb}$[a] (A cm^{-2})	R_0[a] (Ω)
Non-gelled, anodic	1	0.06	1.38×10^{-5}	18.43
	0.5	0.02	9.45×10^{-6}	39.65
Non-gelled, cathodic	0.5	0.09	1.08×10^{-5}	28.84
	0.05	0.05	5.71×10^{-6}	115.47
Gelled, anodic	1	0.05	1.44×10^{-6}	39.65
	0.5	0.02	2.78×10^{-6}	42.44
Gelled, cathodic	0.5	0.08	4.21×10^{-6}	140.47
	0.05	0.04	1.93×10^{-6}	415.85

[a]Calculated on the basis of apparent geometrical area (33 cm^2).

batteries using immobilized electrolyte as it manifests the sum total of the ohmic loses that occur in the pores by pore-plugging and immobilization-induced changes.

Limitations of the model

The quasi-reversibility of the $Pb/PbSO_4$ system assumed in deriving eqn. (11) may not be universally valid, especially for cathodic polarization at an SOC equal to unity. For example, the charging efficiency at this SOC will be very poor and currents passed will be completely utilized for eqn. (2). Similarly, at an SOC close to zero, there is very little amount of lead for the anodic reaction and, hence, during charging, all the faradaic currents will be consumed only for eqn. (1) and departure from quasi-reversibility can be reflected in the initial deviation from linearity in the experimental plots. Variation of R_0 with SOC will not be uniform at these limiting SOC values. Thus, the model is most appropriate close to SOC=0.5, where cathodic as well as anodic schemes indicate mutual validity.

Another important limitation is imposed by neglecting the role of adsorbed hydrogen. The coverage-induced variations of exchange-current densities, capacitance and R_0 values are also not included. This is because eqn. (4) is valid only if the reaction of interest does not involve an adsorbed intermediate or, more importantly, the adsorbed intermediate is not participating in the rate-determining step. This cannot be strictly true as silicate ions are known to adsorb on the electrode surface and, thereby, change the reaction kinetics. Lastly, the effect of adsorption pseudo-capacitance is also ignored in the present analysis.

Inspite of the above limitations, the assumptions involved in the model are quite general for most battery electrodes and the estimation of the internal ohmic drop due to pore-plugging may provide a useful physical insight into the design of maintenance-free batteries. Furthermore, all of the kinetic parameters are obtained by polarizing the electrode less than 10 mV, with negligible SOC change. Hence, the analysis can be considered as a non-destructive method for obtaining useful kinetic data.

Conclusions

A quantitative analysis of potential–time transients of a porous $Pb/PbSO_4$ electrode in gelled and non-gelled sulfuric acid demonstrates numerous key features that are useful for designing maintenance-free batteries. This analysis, despite its non-destructive nature, provides several important kinetic parameters for both the lead and the hydrogen-electrode reactions. Furthermore, the effects of accumulation of non-conducting discharged products, as well as the addition of thixotropic agents in the electrolyte, have been incorporated as resistance parameters by developing a model based on pore-plugging. The study shows that this resistance component can affect significantly the design of maintenance-free lead/acid batteries.

Acknowledgements

The authors are grateful to the late, Professor S. Sathyanarayana of the Indian Institute of Science, Bangalore, for several critical discussions. Financial support from the University Grant Commission, New Delhi, is also acknowledged.

References

1 M. Maju and N. Penazzi, *J. Power Sources, 25* (1989) 99.
2 A.M. Hardman, *J. Power Sources, 23* (1988) 127.
3 J. Sterbe, B. Reichman, B. Mohato and K.R. Bullock, *J. Power Sources, 31* (1990) 43.
4 K. Vijayamohanan, S.N. Joshi and S. Sathyanarayana, *J. Power Sources, 30* (1990) 169.
5 R.M. Lafollette and D.N. Bennim, *J. Electrochem. Soc., 137* (1990) 3693.
6 K. Micka and I. Rousar, *Electrochim. Acta, 29* (1984) 1411.
7 J. Newman and W. Tiedemann, *AIChE J., 21* (1975) 25.
8 D. Pavlov, *Electrochim. Acta, 13* (1968) 2151.
9 D. Pavlov, in B.D. McNicol and D.A.J. Rand (eds.), *Power Sources for Electric Vehicles,* Elsevier, Amsterdam, 1984, p. 113.
10 M.P. Vinod and K. Vijayamohanan, *J. Appl. Electrochem.,* in press.
11 M. Barak (ed.), *Electrochemical Power Sources,* Peter Peregrinus, Stevenage, 1980, p. 290.
12 R. Iler, *The Chemistry of Silica,* Wiley, New York, 1979, p. 287.
13 S. Okazaki, S. Higuchi, N. Kubota and S. Takahashi, *J. Appl. Electrochem., 16* (1986) 513.
14 T.F. Sharp, in A.J. Bard (ed.), *Encyclopedia of Electrochemistry of Elements,* Vol. 1, 1973, p. 308.